A Cooperative Scheme for Spectrum Sensing in Cognitive Radio Systems

Adamant Sula, Chi Zhou
Illinois Institute of Technology, Department of Electrical and Computer Engineering, Chicago, USA
Email: {asula, zhou}@iit.edu

***Abstract*—As wireless communication systems become more and more pervasive, demand for spectrum is following an ever increasing trend. At the same time, studies conducted by governmental bodies show that a considerable part of the allocated spectrum is underutilized. This paper aims to design and develop a cooperative spectrum sensing scheme from a comprehensive perspective including sensing, communication, decision, and transmission along with some other additional features. The scheme is based on dynamic weighting of cooperating users according to their reliability based on historical decision data. The work is articulated into a model development, the definition of mathematical metrics, and rounds of simulations to asses the validity of the model. Simulation results indicate that the model provides an adequate answer to some of the most challenging aspects of cognitive spectrum sensing.**

I. INTRODUCTION

In today's telecommunication world, the continuous diffusion of mobile communication systems results in an ever increasing demand of spectrum. On the other hand, studies conducted by governmental bodies in different countries have shown that spectrum is in reality underutilized [1]. Licensed or primary users (PU), in fact, use the spectrum only during a fraction of the time and also in locations whose span is quite limited as compared to the geographical area the spectrum is licensed for. Hence, it becomes inevitable to develop new spectrum-utilization approaches in which unlicensed users are allowed to use spectrum allocated to licensed users as long as the unlicensed users do not interfere with the licensed users.

Many authors have tackled the problem from different perspectives and suggested cognitive radio as the solution. In cognitive radio research, cooperative spectrum sensing has attracted a lot of attentions, as it is capable of combating the deep fading and shadowing as well as providing sufficient guarantees to PU's prioritized access to licensed spectrum.

Taherpour et al. [2] suggest a cooperative approach where cognitive users (CU) share information regarding eventual presence of licensed users. One of the most relevant aspects of this approach is that CU-s exchange observation information rather than decisions so that each CU combines its own observations with those of other CU-s.

Yu et al [3] analyze the impact of the number of cognitive users on miss-detection probability assuming Rayleigh fading channels and fully-cooperative cognitive users. The paper provides a comparison of the impact of probability of detection as the number of CU-s increases from 2 to 4. It does not however, analyze whether there is an upper bound beyond which further increase in the number of CU-s results in prohibitive processing time increase.

Chen et al [4] analyze the performance of cooperative spectrum sensing in a TDMA environment. The approach consists of the usage of some of the time slots for communication between cognitive users. The analysis takes into account power requirements. One of the main assumptions of this model is that the location of the primary users is known. The limitation is quite relevant if scenarios with large number of cognitive users are considered. Another implication is the reduction of performance due to slotted nature of transmissions in TDMA.

Sun et al [5] focus on the *reporting* aspects of cooperative spectrum sensing. The main assumption in this case is that the reporting channel is Rayleigh fading. Based on this, CU-s are grouped in clusters and the user with the largest channel gain is selected to collect sensing information from all other users in the cluster. The main advantage of this approach is that channel fading is considered as opposed to models assuming ideal channels.

The previous references are representative of some of the directions in which cooperative spectrum is moving in the attempt to identify reliable and performing spectrum sensing schemes [6]-[10]. The fact that different authors approach the problem from different angles and that there are advantages and disadvantages associated with each model is a direct result of the objective complexity of the problem at hand.

In this paper, we aim to design and develop a cooperative spectrum sensing scheme from a comprehensive perspective including sensing, communication, decision, and transmission along with some other additional features. The work is articulated into a model development, the definition of mathematical metrics, and rounds of simulations to asses the validity of the model. Simulation results indicate that the model

Manuscript received April 30, 2009; revised August 15, 2009; accepted August 03, 2009.

doi:10.4304/jcm.4.10.741-751

provides an adequate answer to some of the most challenging aspects of cognitive spectrum sensing.

II. COOPERATIVE SENSING MODEL

In the attempt to provide a solution to some of the issues that intrinsically characterize spectrum sensing, a cooperative scheme is suggested. The following sections highlight the framework definition in a step-by-step way. The idea is to explain different aspects of the proposed solution starting from a simple scenario and expanding, little by little, so that more generality is added through introduction of additional analytical layers.

A. Time Fragmentation

Unlike traditional radio, Cognitive Radio (CR) users are able to sense the spectrum before transmitting in order to avoid interfering with primary users. Fig. 2-1 below shows the suggested breakdown of a time cycle.

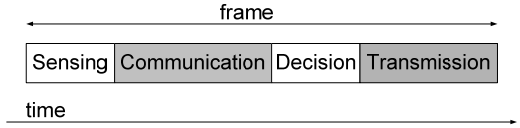

Figure 2-1. Generic time-fragmentation scheme

- Sensing

Basically, the CU starts by sensing the spectrum in order to assess the presence (or lack of it) of other users (primary or cognitive) using the spectrum. The quantitative result of this step represents the input of the subsequent stage.

- Communication

During this stage each CU communicates the result of the *sensing* stage with other CUs. As a result, each CU obtains the sensing results of (potentially all) other CUs in the time-frequency-space constellation.

- Decision

During this stage, the core of the spectrum sensing analysis is carried out. The decision logic takes into account *self*'s sensing results and the sensing results received from other CUs (if any) during the *communication* stage.

- Transmission

Data transmission is subject to the results of the *decision* step. In case of favorable decisions, data are transmitted during the transmission window.

B. Sensing Stage

During this stage, the presence or absence of other users in the frequency band of interest is assessed using an energy detector. As a direct result of this, *sensing* is performed based on an approach that allows considerable reduction of the sensing time due to the simplicity of the scheme itself. The output of the energy detector is then used to assess the presence (or lack of it) of other users and the decision regions are mapped with a bit-pattern representation. Given that at least two bits need to be used, anyway, the energy detection scheme becomes as shown in Fig. 2-2. For values inside the uncertainty region the measurement is reported to other cooperating CU-s. In case of measured values outside the uncertainty zone, a zero/one value is reported to other CU-s.

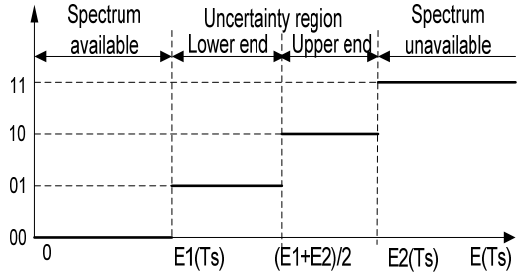

Figure 2-2. Enhanced energy detection quantization

C. Communication Stage

During this stage, cognitive users exchange information regarding the results of the *sensing* stage. This information is clearly different from any actual data exchange between the nodes. Namely, each cognitive user reports thus either the "certain" presence/absence of other users or the measured energy value. This distinction has several implications in terms of the CR system behavior and performance.

(a) Channeling

In this scheme, the exchange of sensing results is performed using a channel with a very large band as shown in Fig. 2-3 below. Ultra Wide Band (UWB) transmission can reduce the interference significantly as the interference generated by the signal spread over a very large band can be treated essentially as noise. On the other hand, synchronization requirements are relaxed considerably.

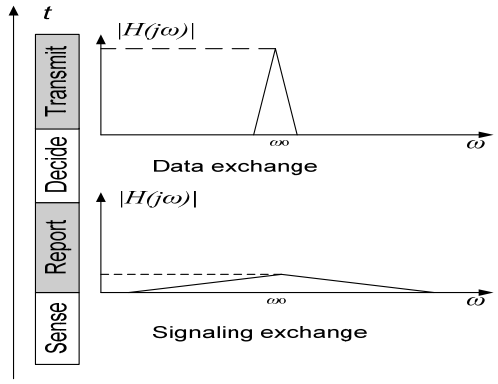

Figure 2-3. Ultra Wide Band signaling exchange

The main drawback of this exchange modality consists of the increased complexity of the transmitter and receiver at each CU end. The other drawback stems from power limitations associated with UWB transmissions. Regarding the latter aspect, two things are to be considered. First, UWB communications are only used for signaling when operations at very low bit rates are acceptable. Secondly, range increase can be ensured either through recourse to multi-finger Rake receivers

[12] or adoption of pulse repetition cycle techniques allowing interference minimization while not reducing the UWB average signal power [13]. Thus, UWB is used for signaling since the advantages of reduced interference and relaxed synchronization requirements are considered to outweigh the drawbacks deriving from increased complexity.

(b) Synchronization

The CU operations are to be characterized by a clear distinction of signaling exchange and data transfers. Since buffering of results received from other nodes is anyway necessary and considering that UWB signaling is preferred to in-band signaling, non-synchronized parallel frames are used as illustrated in Fig. 2-4. With this new frame structure, *sensing* and reporting of sensing results follow independent cycles as compared to the *decision* and *transmission* stages as shown in Fig. 2-5.

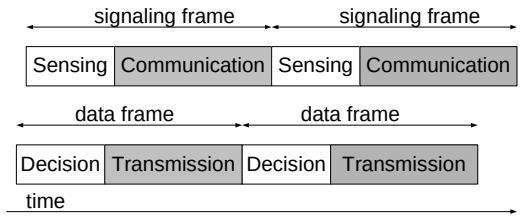

Figure 2-4. Non-synchronized, parallel frames

The CU senses the spectrum over a predefined time interval. At the end of this interval a comparison between the current measurement and measurements of the previous sensing rounds are performed. This is done to ensure that signaling data are transmitted differentially. *Self* sensing results are used during the decision map update. Similarly, the CU "listens" to cooperative sensing information provided by other CU-s. Whenever some information is received from other CU-s the decision map is updated accordingly. The point-in-time decision map is used during the decision stage of actual data transmission flow. Depending on the *decision* result, data are either transmitted over the unlicensed channel or the transmission round is skipped.

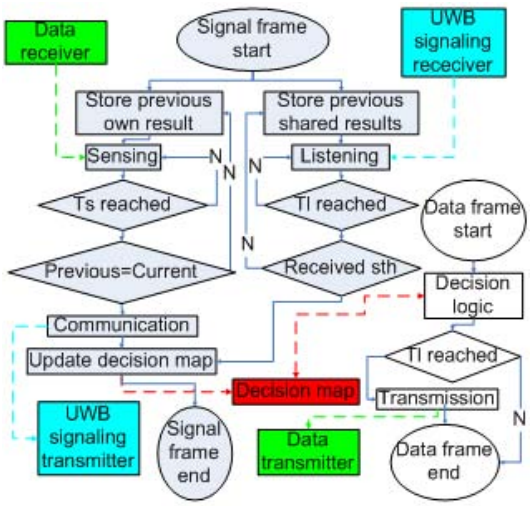

Figure 2-5. CU with parallel frames

As a corollary to the above considerations, signaling and data frames of the CU shown in Fig. 2-4 are characterized by two sets of dynamic, non-synchronized frames. The length of the segments composing the frames is discussed later on in this paper. The adoption of non-synchronous parallel frames has the following implications:

1. *Sensing* time and *communication* time do not influence the system throughput as both tasks are performed independently of actual data transmissions.

2. The signaling part of the *communication* stage needs to be based on an architecture that allows simultaneous transmission and reception

3. In contrast to the traditional radio scenario, *transmission* time can be only reduced by the *decision* time.

D. Decision Stage

This is where the sensing results of the *self* and those of the cooperating CUs are combined together and evaluated in order to determine whether the spectrum is vacated from the PU-s. The decision is obtained as a weighted sum of the decisions of the *self* and those of the other CUs:

$$d = w_0 d_0 + w_1 d_1 + ... + w_m d_m = \sum_{i-0}^{M} w_i d_i \quad (2\text{-}1)$$

where d_i is the *n*-bit representation of the output of the energy detector of the i^{th} CU (i=0 for *self*) and w_i are the associated weights, respectively.

As indicated in Eq. (2-1), the scheme is based on two assumptions:

- distinction between PU-s and CU-s
- distinction between CU-s

Since these differentiations can not be accomplished by the energy detector, the suggested approach is to use MAC-layer protocols capable of differentiating between PU-s and CU-s and uniquely identifying CU-s.

While individual decisions are the results of the energy detection stage, the assignment of the weighting coefficients is performed dynamically during the *decision* stage based on the following considerations:

1. The weight assigned to a CU is proportional to the degree with which this CU has been reporting reliable results during the past frames. Reliability is measured as the inverse of the difference between the individual d_i provided by the CU and the final decision made by the *self*. From now on, we will denote current values with $x(k)$ and past values with $x(k-t)$ where $t = 1,2,...$ Based on this, the point-in-time reliability of the results reported by a given CU is given by

$$r = \begin{cases} 1 & d(k) = d_i(k) \\ 0 & |d(k) - d_i(k)| = 1 \\ d_i(k) & d(k) = 1 \\ 1 - d_i(k) & d(k) = 0 \end{cases} \quad (2\text{-}2)$$

Typically, reliability schemes are based on SNR values assuming that CU-s with higher SNR should be granted

higher weights. This approach works well in case of centralized decisions. However, in this model, each CU performs decisions locally therefore SNR-based weighting is not applicable mainly because high SNR values do not guarantee that the cooperating CU-s is in a better position to sense the spectrum than other CU-s. On the other hand, the definition of Eq. (2-2) is potentially prone to race-condition errors. However, considering that reliability values are averaged over I iterations (I is the depth of the reliability registry in the decision map) the upper bound for the probability of a divergent CU is given by

$$\hat{div}\, Pi \le 2^{-I} \tag{2-3}$$

which represents the probability of I consecutive wrong decision on a CU in a worst-case scenario.

Based on Eq. (2-3), the overall system diverging probability bound is given by

$$\hat{div}\, P = \bigcap_{i=1}^{N} \hat{div}\, P_i \le 2^{-IN} \tag{2-4}$$

The probability of a divergent CU can thus be kept sufficiently low by increasing the registry depth even in case of very few cooperating CU-s. For instance, when $N = 2$, setting $I = 5$ results in

$$\hat{div}\, P < 0.001$$

The weight assignment relationship is as follows

$$w_i(k) = \Psi(r_i, I) = \frac{\sum_{i}^{I} r_i(k-i)}{I} \tag{2-5}$$

and the normalized weights are given by

$$\overline{w_i} = \frac{w_i}{\sum_{j=1}^{M} w_j} \tag{2-6}$$

where M is the point-in-time number of CUs and the overall decision calculated as follows

$$D = \sum_{i=0}^{M} \frac{d_i \sum_{i=1}^{I} r_i(k-i)}{I \sum_{j=1}^{M} w_j} \tag{2-7}$$

2. The final decision is made taking into account *self*'s detection thresholds *E1* and *E2* as illustrated in Fig.2-2. Based on this, the decision output is calculated based on the following relationship

$$D = \begin{cases} 1 & d > E2 \\ 0 & d < E1 \\ uncertain & otherwise \end{cases} \tag{2-8}$$

3. In case of uncertainty, the decision is recalculated. Since the CUs who report same values over time are more likely to be reporting correct data, the number of consecutive decisions of same value for each CU is stored. During the recalculation, the CU with the lowest value of consecutive decisions of same value is excluded from the calculation. In case of a tie, the CU with the result which is further away from the *(E1+E2)/2* point is used. If there still is a tie, one of the CUs is excluded randomly. The procedure described here is repeated until the calculated decision value falls outside the uncertainty range.

4. In case the energy detection of the scheme results in a hard decision of 0, weighting is performed based on the algorithm described in the previous section

5. In case the energy detection scheme results in a hard decision of 1, the *self* decides that there is no spectrum available and the decision in this sense is made right away.

CU id	Decision	Counter	Hist. reliability		
Id bits	*n* bits	6 bits	R(k-1)	…	r(k-*I*)
0…0	00…10	0000001	0.15	…	0.13
0…1	11…11	0000110	0.71	…	0.43
0..10	10…01	0001001	0.82	…	0.14
0..11	00…11	0000001	0.12	…	0.54
0.100	10…10	0000110	0.24	…	0.02
0.101	11…10	0000111	0.92	…	0.33
0.110	00…00	0000110	0.23	…	0.24

Figure 2-6. Decision map structure

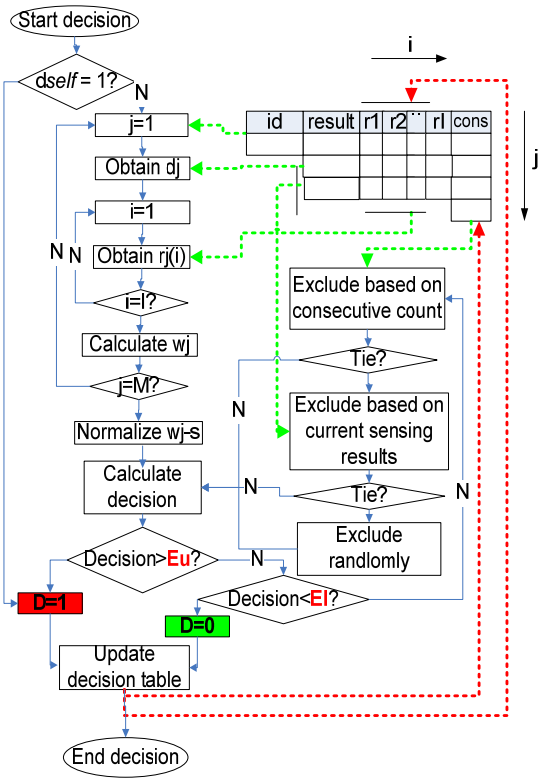

Figure 2-7. Decision logic

The decision map structure contains information regarding the CU identifier, the current energy detection result, and a series of historical weights stored in a FIFO

shift-register of depth *I* as shown in the example of Fig. 2-6. The flowchart of Fig. 2-7 summarizes the modalities with which the decision map is used and maintained during the *decision* stage.

The decision table is updated after each decision round. Likewise, the upper and lower bound are modified depending on the stage of the threshold validation logic. In fact, the initial verification is performed using *E1* and *E2* as evaluation criteria. In case of uncertainty, the upper and lower bound are drawn closer to the *(E1+E2)/2* point and the decision table reduced through exclusion of the less significant entry. This is repeated until only one entry is left in the decision table. In that case, the decision is made based on the energy value of that entry as compared to the *(E1+Eu)/2* point.

Table 2-1 below represents an example of how the decision map is dynamically updated.

Table 2-1. Weight calculation scheme

Step	Map*				E1	Eu	R	D
	Id	C	M	W				
	1	4	6	0.25				
1	2	3	12	0.25	2	20	10.75	?
	3	4	9	0.25				
	4	4	16	0.25				
	Id	C	M	W				
	1	4	6	0.33				
2	2	**3**	15	**0.0**	4	18	10.33	?
	3	4	9	0.33				
	4	4	16	0.33				
	Id	C	M	W				
	1	4	6	0.5				
3	2	3	15	0.0	4	18	11	?
	3	4	**9**	**0.0**				
	4	4	16	0.5				
	Id	C	M	W				
	1	4	6	**0.0**				
4	2	3	15	0.0	4	18	16	1
	3	4	9	0.0				
	4	4	16	1				

* *C*-counter, *M*-measurement, *W*-weight, *R*-result, *D*-decision

D. Transmission Stage

The transmission stage is considered to be handled based on the traditional radio approach. In fact, once the *decision* logic determines that the band is vacated, the CU can use the band as if it were a licensed PU. This only applies to a limited time duration which is denoted by T_T. At the end of this interval, a new decision cycle starts. Assuming that the decision time is given by T_D, the throughput efficiency ratio is given by

$$\eta = \frac{T_T}{T_T + T_D} \tag{2-9}$$

Eq. (2-9) highlights the presence of the tradeoff between throughput and accuracy (i.e., probability of false alarm and probability of missed detection). It is clear, from the flow chart of Fig. 2-7, that the number of operations during the decision logic implementation will increase in case of repeated uncertain decisions. This means that increasing the reliability of the decision comes at the cost of more operations and hence an increase in the decision time. Such an increase would have a negative impact on the throughput efficiency ratio.

Another thing to note regarding the transmission is that the maximization of the transmission time for a given CU does not guarantee a maximization of the system throughput. Consequentially, specific and distinct metrics are required for the CU-related and overall system performances.

III. SYSTEM PERFORMANCE METRICS

During the description of the model several parameters have been introduced and described. In this section, the role of these parameters is summarized. Moreover, some system metrics are defined in the attempt to render the system performance measurable and hence set the basis of the analytical model to be used during the simulations.

A. Probability of Missed Detection (PMD)

PMD represents the errors that would occur in case the presence of a PU is not detected and a given CU wrongly considers the band to be vacated. This would result in interference which is obviously an undesired result. Considering that cooperative sensing is used, the PMD can be described as

$$PMD_i = P_i(E_i < E1 \mid PU_j) \tag{3-1}$$

where $P_i(E_i < E1 \mid PU_j)$ is the probability that the CU does not sense any transmission from PU-s though a primary user is present transmitting. Since an energy detector is used, the energy can be shown [11] to have a non-central chi-square distribution of the form $E_i = \chi^2_{2u}(2\gamma_i)$ where γ_i is the point-in-time SNR and $u = T_S W$ where T_S and W are the sensing time and signal bandwidth, respectively. Based on this, the PMD for a CU is given by

$$PMD_i = 1 - Q_u(\sqrt{2\gamma_i}, \sqrt{E1}) \tag{3-2}$$

where Q_u is the generalized Marcum Q-function. Seen from a system perspective, the probability of missed detection is given by

$$PMD = \bigcup_{i=1}^{N} PMD_i \tag{3-3}$$

or

$$PMD = \bigcup_{i=1}^{N} (P_i(E_i < E1 \mid PU_j) \tag{3-4}$$

where same upper energy detection level is assumed for all CU-s.

This metric represents a way of assessing the reliability of the CR system in terms of its capability to ensure seamless integration with traditional radio PU-s unaware of the presence of unlicensed CU-s.

B. Probability of False Alarm (PFA)

PFA represents the errors that would occur in case a band is erroneously considered to be occupied by a PU. This would result in one transmission round being unnecessarily skipped with a consequential negative impact on the system performance in terms of data transmission rates. Considering the cooperative sensing scheme being used, the PFA can be formulated as

$$PFA_i = P_i(E_i > E2 \mid \overline{PU}) \quad (3\text{-}5)$$

where $P_i(E_i > E2 \mid \overline{PU})$ is the probability that the cognitive users assumes transmission from primary users though there is no PU present transmitting. In this case the energy has a central chi-square distribution [11] and the PMD for each CU can be expressed as

$$PFA_i = \frac{\Gamma(u, E2/2)}{\Gamma(u)} \quad (3\text{-}6)$$

where $\Gamma(u,E)$ and $\Gamma(u)$ are the incomplete gamma and gamma functions, respectively.

From a system perspective, the probability of false alarm is given by

$$PFA = \bigcup_{i=1}^{N} PFA_i \quad (3\text{-}7)$$

or

$$PFA = \bigcup_{i=1}^{N} (P_i(E_i > E2 \mid \overline{PU}) \quad (3\text{-}8)$$

Since the probability of transmission of the primary user is given by

$$PU = \bigcup_{j=1}^{M} PU_j \quad (3\text{-}9)$$

Eq. (3-8) can also be written as

$$PFA = \bigcup_{i=1}^{N} (P_i(E_i > E2 \mid \bigcap_{j=1}^{M} \overline{PU}_j) \quad (3\text{-}10)$$

This metric represents a way of assessing the quality of the CR system in terms of its capability to ensure transmission rates that allow practical utilization of the CR system as an alternative for spectrum acquisition.

C. Cognitive User Throughput (CUT)

This metric represents the amount of data that the CU can transfer per unit of time. Elevated throughput values are obviously desired. Clearly, the decision time needs to be kept as low as possible while not being detrimental to appropriate control on PMD and PFA values. Considering the cooperative sensing being used, the throughput can be written as

$$TU_i = \sum_{k=0}^{K} {}_iT_k \quad (3\text{-}11)$$

where K represents the number of transmission cycles and ${}_iT_k$ denotes the throughput of a transmission cycle. Because of the duplication of the CU logic in sensing and data communication as described in Fig. 2-7, *transmission* and *decision* follow different trends. This becomes evident if *decision* and *communication* are considered in terms of time units. Assuming that, at any time, the sensing cycle is given by

$$TC_i = TS_i + TT_i \quad (3\text{-}12)$$

It follows that longer decision time results in reduced transmission time, regardless of the timeframe length being used as a reference (system clock, 1 sec, etc…).

D. Cognitive System Throughput (CST)

This metric differs from the CUT in that it takes into account the overall system performance as opposed to the performance seen from the perspective of a single CU. Regarding this, it is reasonable to expect opposite trends regarding the two metrics. Although the suggested sensing scheme is cooperative, the idea behind the CU cooperation is to ensure more accurate decisions. On the other hand, decision accuracy is something CU-s pursue in the attempt to achieve better performance metrics. A given CU, as such, is not in the position to evaluate whether this is something that results in better overall system performance. Because of this unawareness, CUs operate selfishly. Consequentially, there is no guarantee of alignment between the values of a given metric at the CU level and the corresponding system-wide values. The overall system throughput is given by the sum of all individual throughputs

$$T_{SYS} = \sum_{i=1}^{N} TU_i = \sum_{j=1}^{N} \sum_{k=0}^{K_j} {}_iT_k \quad (3\text{-}11)$$

where N is the number of cooperating CU-s.

It is important to notice that the number of transmission cycles varies across CU-s. This is emphasized by indexing the upper limit of the inner summation of the previous equation. Clearly, the number of transmitting cycles depends on the presence (or lack thereof) of PU-s and also on the duration of the *decision* stage.

IV. SIMULATION

The formulas of the previous section provide the analytical result of the expected system behavior in terms of metrics. However, because of the complexity of the model and the fact that the metrics are not independent, a simulation setup is necessary in order to assess the validity of the model. The following sections describe the setup and related assumptions, some of the simulation parameters and their relationship to the cooperative sensing model, and the results of the simulation.

A. Simulation Setup

The simulation assumes a variable number of CU-s and PU-s that can be randomly located in a fixed-length square grid. The grid size is set to 1 km x 1 km with PU-s and CU-s distributed randomly in the grid. PU frequency assumed at 900 MHz. UWB signaling transmission power assumed in the boundary of allowed interference level -40dBm. PU channel size *W* and time of sensing

assumed to result in time-band product values of $u = T_S W = 4$. The assumption is that cognitive users can communicate with each other regardless of their location inside the grid.

The path los model used in the simulations is as follows:

$$PL(d) = \bar{P}\,L(d_o) + 10\,n\log\left(\frac{d}{d_o}\right) + X_\sigma \qquad (4\text{-}1)$$

where X_σ is a zero-mean Gaussian variable and, assuming operations in urban area for cellular radio, $n = 4$ is used.

Regarding the definition of the lower and upper bound detection thresholds, considerations regarding the percentage of coverage area are used. To this end, assuming a CU at a distance d from the PU transmitter the percentage of coverage over a given threshold γ is given by

$$U(\gamma) = \frac{1}{\pi R^2}\int_0^{2\pi}\int_0^{R} \Pr\left[P_r(r) > \gamma\right] r\,dr\,d\theta \qquad (4\text{-}2)$$

The energy detection levels are set based on the received power settings of Fig. 4-1 below.

PU dist.	Received Power	Coverage	Description
100m	0 dBm	100%	Ref distance
500m	-30 dBm	80%	Upper bound criterion (E1)
1500m	-40 dBm	66%	Lower bound criterion (E2)

Figure 4-1. Power coverage settings

Regarding the location of the users in the simulation grid, there are no limitations as to their relative or absolute position. All users can be stationary or mobile. In case of mobility, the assumption is that the users random-walk inside the grid at low speeds. In order to make the simulation more realistic, additional shadowing is also included in the simulation logic as illustrated in Fig. 4-2 below.

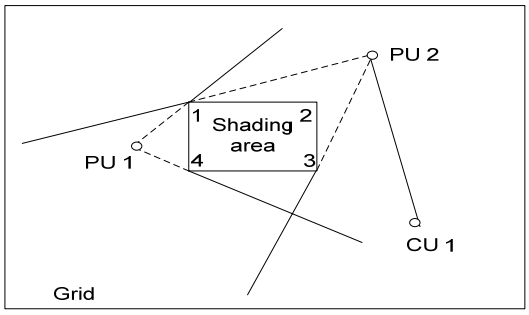

Figure 4-2. Primary user shadowing

In this scope, additional shadowing calculations are performed based on geometrical line-of-sight considerations. PU-s are considered to be shaded with respect to a CU if located in the shadowing cone projected by the shadowing area as shown in the previous figure

The assessment of additional shadowing is performed based on angle calculations. For CUs in the sector of PU2 (forward shadowing cone), the shadowing condition is given by

$$Min\,(\angle PU_j - x) < (\angle PU_j - CU) < Max\,(\angle PU_j - x)$$

For CU-s in the sector of PU1 (reverse cone), the calculation is inverted and the shadowing condition is given by:

$$Min(\angle PU_j - x) > (\angle PU_j - CU) > Max(\angle PU_j - x)$$

If both the primary users and cognitive user are inside the shadowing area, the primary user is considered to be under additional shadowing.

B. Simulation Results

This section summarizes the result of a large number of simulation runs. The simulation data relate to the system metrics describes in the previous sections.

Number of CUs

Fig. 4-3 provides a comparative overview of both cooperating and non-cooperating schemes in case of simulations with different number of CU-s. Simulation results indicate that, on average, an improvement of 80% is obtained as compared to the non-cooperative scheme.

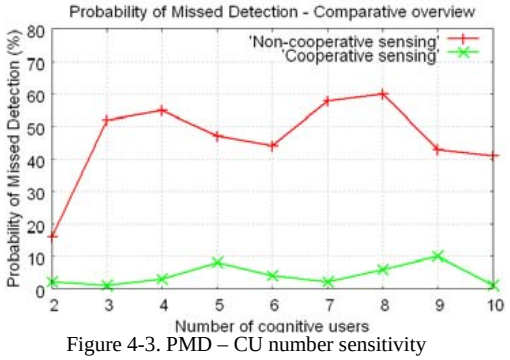

Figure 4-3. PMD – CU number sensitivity

The reduction of the PMD in the cooperative case, however, comes at the price of an increased PFA as shown in the diagram of Fig. 4-4 below.

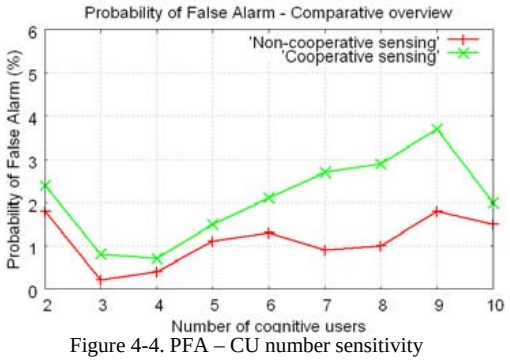

Figure 4-4. PFA – CU number sensitivity

Quite importantly, both schemes provide a similar PFA trend and the cooperative scheme performance is not far behind the non-cooperative one if absolute PFA values are considered.

Fig. 4-5 provides a summary of the overall system performance in case of cooperative sensing. It summarizes system behavior in terms of the PMD, PFA and throughput efficiency. The diagram indicates that reduced PMD while keeping the PFA reasonably low still allows operations at acceptable throughput efficiency levels. However, the diagram also indicates variations of throughput efficiency of as high as 25%.

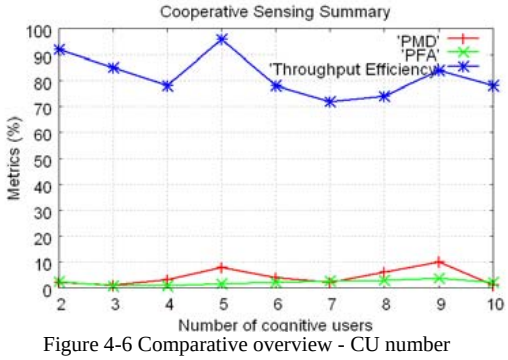

Figure 4-6 Comparative overview - CU number

Assuming worst-case scenarios, the diagram shows that the scheme hits a limit if throughput efficiency values above 70% are to be ensured regardless of the number of cooperating CU-s

Number of PU-s

Fig. 4-6 provides a comparative overview of both cooperating and non-cooperating schemes in case of simulations with different number of PU-s. Simulation results show that, on average, an improvement of approximately 98% is obtained with respect to the non-cooperative scheme.

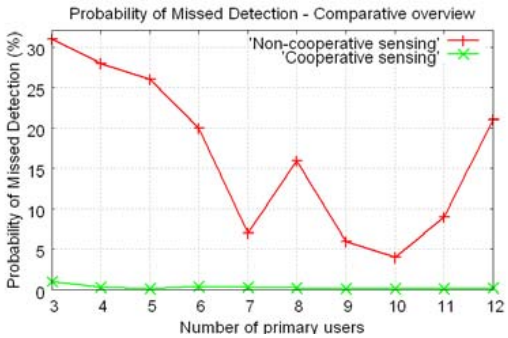

Figure 4-6. PMD – PU number sensitivity

As the previous diagram shows, the cooperative scheme provides a detection mechanism which is not sensitive to variations in the number of PU-s. This makes the scheme a good candidate for deployment in operating contexts characterized by elevated PU density.

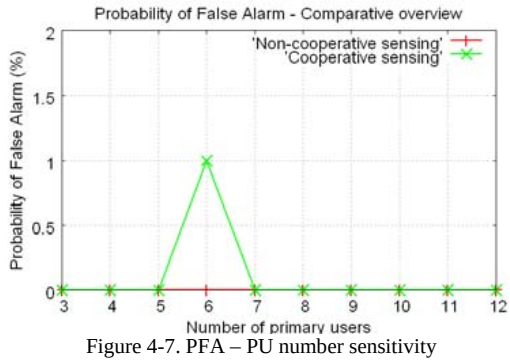

Figure 4-7. PFA – PU number sensitivity

Regarding the PFA, unlike the previous simulation rounds, the cooperative scheme offers practically the same performance as the non-cooperative one. Fig. 4-7 provides an overview of both cooperative and non-cooperative schemes. In this specific case, the behavior of both schemes is practically the same in PFA absolute value terms.

The diagram of Fig. 4-8 provides a graphical illustration the PMD, PFA and throughput as the number of PU-s varies.

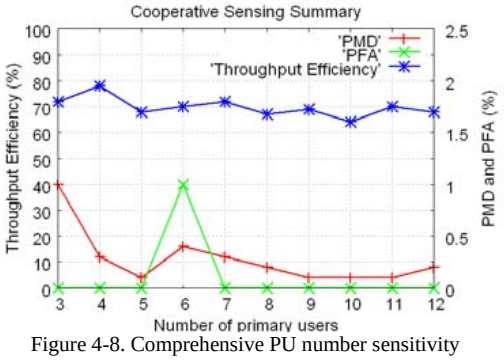

Figure 4-8. Comprehensive PU number sensitivity

From a comparison with Fig. 4-5, it emerges that the cooperative scheme is less sensitive to variations of the PU number as compared to the CU one. The scheme is characterized by very low PMD and PFA and stable throughput efficiency at 70%.

Shadowing Area Size

Fig. 4-9 provides a comparative overview of the PMD for both cooperating and non-cooperating schemes in case of simulations with different relative shadowing area sizes.

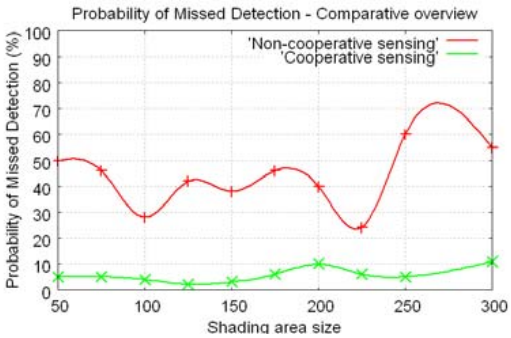

Figure 4-9. PMD – Shadowing area size

On average, an improvement of at least 80% is obtained and PMD values of less than 11% are ensured.

Regarding the PFA, Fig. 4-10 shows that both schemes follow a similar a pattern. As combined with the considerations of the previous point, the scheme offers good handling of PMD reduction, but is exposed to elevated PFA values.

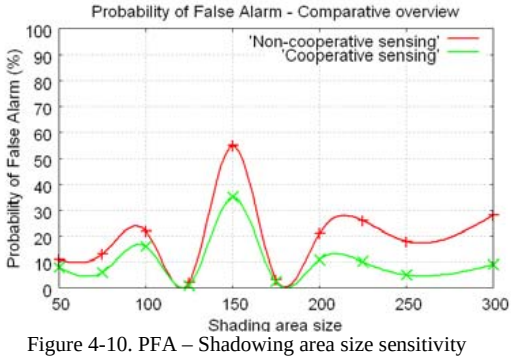

Figure 4-10. PFA – Shadowing area size sensitivity

The diagram of Fig. 4-11 below shows that the throughput efficiency oscillates at around 80%. This also indicates that 20% of the data communication cycle is spent on *decision* cycles.

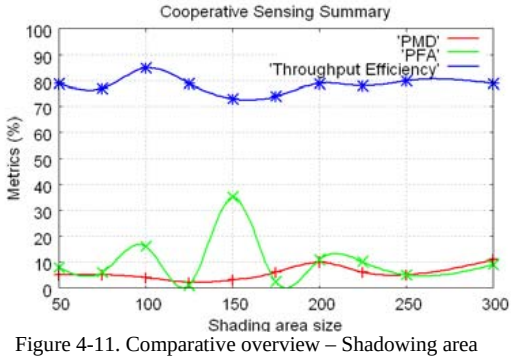

Figure 4-11. Comparative overview – Shadowing area

The tradeoff between accuracy (low PMD) and transmission efficiency (throughput) is, in this case evident. Considering the three metrics, it can be concluded that the cooperative scheme offers a good option if applied in environment with elevated PU density where data exchange rates are not very elevated.

Mobility

In these simulation rounds, both CU-s and PU-s are considered to be mobile. Users move inside the grid at around 20-30 km/h and they change their location based on random walk. In all simulations CU-s and PU-s are configured to have same mobility speed. Fig. 4-12 above illustrates the PMD behavior of the cooperative scheme. The diagram highlights that mobility values have relatively limited influence on PMD handling.

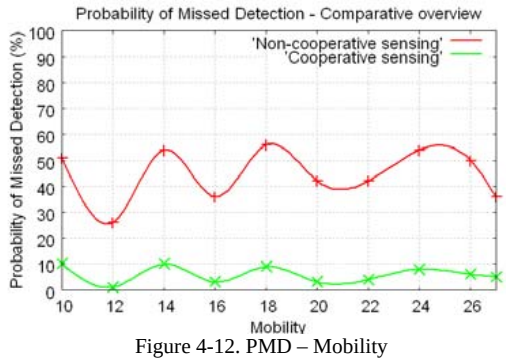

Figure 4-12. PMD – Mobility

Fig. 4-13 summarizes the comparative overview in case of PFA handing. Cooperative PFA absolute values are very close to non-cooperative ones.

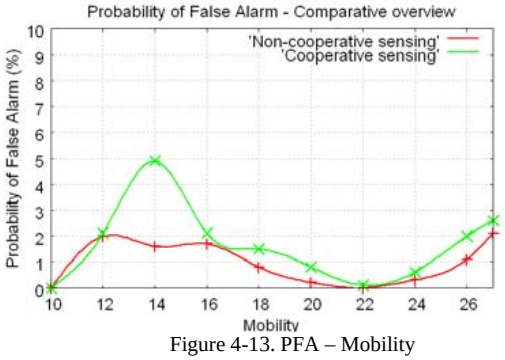

Figure 4-13. PFA – Mobility

The previous diagram also indicates that the PFA is minimized for mobility in the range 20 to 24 which corresponds to a speed of approximately 20-30 km/hour.

Fig. 4-14 provides an illustration of the cooperative scheme behavior in terms of PMD, PFA and throughput efficiency. The scheme has an average throughput efficiency of 75%.

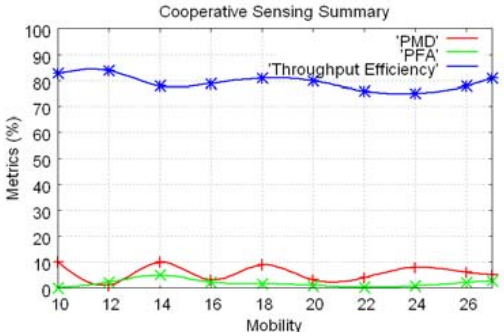

Figure 4-14. Comparative overview – Mobility

It is also possible to see that the cooperative scheme exhibits a stable pattern regarding all metrics as the mobility variable varies in a wide interval.

C. Comparison with Other Cooperative Scheme

The figures and considerations of the previous section relate to comparison of results with the non-cooperative case. This section contains some notes regarding comparison of the suggested scheme with models suggested by other authors.

The model suggested by Saad et al. [15] has been selected due to similarities in the simulation setup and hence relative commensurability of results. In order to compare the PMD and PFA performance of the two schemes, we introduce the concept of CU density. This is expressed as the point-in-time number of users per unit of geographical area under observation (expressed in km^2) as follows

$$\delta_{cu} = M / A \qquad (4\text{-}3)$$

In our case, $A = 1km^2$ and $2 \le M \le 10$ so that $2 \le \delta_{cu} \le 10$ whereas in [15] the simulation is based on $A' = 9km^2$ and $1 \le M' \le 30$ with a CU density in the range $0.1 \le \delta'_{cu} \le 4$ which indicates the presence of some overlap. In a similar way, we consider commensurability of the results based on the number of PU-s. In [15] one PU located at the center of the simulation area is used. This is quite different from our simulation where a variable number of PU-s is used. However, Figs. 4-6 and 4-7 emphasize the relative insensitivity of the scheme behavior with respect to the number of PU-s. Consequentially, assuming 1 PU-s in our simulation same PU-density values as in [15] are obtained.

- Probability of Missed Detection

Simulation results in [15] report a PMD reduction by 86.6%. In our rounds of estimations, a PMD reduction of approximately 90% is achieved. Considering that the simulation setups are not identical, PMD reduction capabilities as such are similar for both schemes.

- Probability of False Alarm

Authors in [15] adopt an approach where system metrics are observer by keeping PFA values constant at 0.1. Fig. 4-4 above however shows that PFA values do not exceed 0.05 in our simulations where the number of CU-s varies. Combined with previous considerations regarding the PMD, this indicates better PFA handling performance than [15] at similar levels of PMD.

- Throughput efficiency

Throughput efficiency data are not available in [15] therefore direct comparison with our scheme is not applicable. However, considering the fact that lower PFA values are likely to lead to higher throughput efficiency there is reason to believe that our scheme would, in a worst-case scenario, perform similar to the scheme of [15].

V. SUMMARY and CONCLUSIONS

Because of the random nature of some of the parameters that influence the simulated behavior of CU-s and PU-s, several simulation rounds are needed. In any case, the cooperative spectrum outperforms the non-cooperative scheme. This relates to both favorable and adverse simulation scenarios.

A. System Metrics

Regarding the system metrics defined in Section 2, the results of the simulations are quite positive. In fact, different design parameters jointly contribute in optimizing the terms of the tradeoffs between PMD, PFA and throughput efficiency.

- Probability of Missed Detection

In terms of absolute values, the scheme exhibits an average value of approximately 4% of PMD. On average, the cooperative scheme under analysis ensures an improvement in the PMD reduction by approximately 90% as compared to the non-cooperative scheme.

- Probability of False Alarm

In terms of absolute values, the scheme exhibits an average value of approximately 2% of PFA.

On average, the PFA-related performance is degraded by 100% as compared to the non-cooperative scheme.

- Threshold Efficiency

On average the cooperative scheme ensures operations at approximately 80% of throughput efficiency. Decision processing takes 20% of useful transmission cycles.

B. Model Parameters and Applicability

Regarding potential characteristics of the cooperative scheme, the following have emerged after several simulation rounds:

- Number of PU-s

System metrics indicate improved performance when the number of primary users in the simulation grid increases. This makes the scheme useful in applications that entail operations in areas characterized by elevated PU density such as densely-populated urban areas.

- Number of CU-s

With the exception of increased decision times, there are no indications of system reliability being affected by an increase in the number of primary users. System metrics indicate very good performance even in case of low CU density.

- Shadowing

As the percentage of shaded area with respect to the simulation grid increases, system metrics indicate increasingly improved performance as compared to the non-cooperative spectrum. This makes the scheme a good candidate in the way to the mitigation of the “hidden terminal” problem.

- Mobility

System metrics are quite reassuring in case of both low and high mobility rates. The model performs best in the range of PU and CU mobility rates of approximately 20-30 km/h. Combined with previous considerations regarding shadowing and PU density, this also witnesses in favor of potential use in vehicular communications in densely-populated urban areas.

Simulation results indicate that one of the most important characteristics of the scheme is better handling of PMD reduction. Regarding this, the 4% PMD that the scheme can achieve does represent a considerable step forward as compared to the non-cooperative case (average values of 40% PMD observed in simulations).

The relative PFA increase could be considered acceptable taking into account the fact that throughput efficiency values for useful transmission cycles are

anyway elevated. In any case, the scheme could be used in applications where requirements regarding data exchange rates are not overly compelling.

REFERENCES

[1] Federal Communications Commission, "Spectrum Policy Task Force, " Rep. ET Docket no. 02-135, Nov. 2002.

[2] A. Taherpour, M. Nasiri-Kenari, and A. Jamshidi, "Efficient Cooperative Spectrum Sensing in Cognitive Radio Networks," in *Proc. IEEE Symp. Personal, Indoor and Mobile Radio Communications*, Athens, Greece, Sep. 3-7, 2007, pp. 1-6.

[3] Z. Yu, Y. Wen-dong and C. Yue-ming, "Cooperative spectrum sensing technique," in *Proc. IEEE Int. Wireless Communication, Networking Conf.*, Sep. 21-25, 2007, pp. 1167-1170.

[4] Q. Chen, F. Gao, A.Nallanathan, and Y. Xin, "Improved cooperative spectrum sensing in cognitive radio," in *Proc. IEEE Vehicular Technology Conf.*, Singapore, May 11-14, 2008, pp. 1418-1422.

[5] C. Sun, W. Zhang and K. Ben Lataief, "Cluster-based cooperative spectrum sensing in cognitive radio systems," in *Proc IEEE Int. Conf. Communications.*, Glasgow, Scotland, UK, June 24-28, 2007, pp. 2511-2515

[6] W. Wang, L. Zhang and Z. Zhou, "On the distributed cooperative spectrum sensing for cognitive radio," *in Proc. Int. Symp. Comm. Inform. Technologies*, Sydney, Australia, Oct 17-19, 2007, pp. 1496-1501.

[7] F. Tian and Z. Yang, "A New Algorithm for Weighted Proportional Fairness Based Spectrum Allocation of Cognitive Radio," *in Proc. 8th Int. Conf. Soft. Eng., Art, Intelligence, Networking*, July 30, 2007, pp. 531-536.

[8] C. Ruiliang, J. Park, and K. Bian, "Robust distributed Spectrum Sensing in Cognitive Radio Networks," in *Proc. IEEE Conf. Computer Communications*, Apr 13-18, 2008, pp. 1876-1884.

[9] H. Sun , J. Jiang, and M. Lin, "Adaptive Cooperation Algorithm for Cognitive Radio Networks," in *Int. Conf. Wireless Communication, Networking*, Sep 22-24, 2006, pp. 1-4.

[10] T. Yiicek and H. Arsalan, "Spectrum Characterization for Opportunistic Cognitive Radio Systems," in *Proc. EEE Military Comm. Conf.*, Washington, DC, USA, Oct 23-25, 2006, pp. 1-6.

[11] V. I. Kostylev, "Energy detection of a signal with random amplitude," in *Proc. IEEE Int. Conf. Commun.*, New York, Apr 28- May 2, 2002, pp. 1606-1610.

[12] R. M. Buehrer, et al., "Range Extension for UWB Communications," retrieved from *http://www.mprg.org/people/buehrer/ultra/pdfs/Range%20Extension%20for%20UWB.pdf* on July 25, 2009

[13] K. Ohno and T. Ikegami, "Interference Mitigation technique for Coexistence of Pulse-Based UWB OFDM," *Journal of Wireless Communication and Networking*, 2008, 11 pgs.

[14] C. Cordeiro and K. Challapali, "C-MAC: A cognitive MAC Protocol for Multi-Channel Wireless Networks," *International Symposium in New Frontiers in Dynamic Spectrum Access Networks*, 2007.

[15] W. Saad, Z. Han., et al., "Coalitional Games for Distributed Collaborative Spectrum Sensing in Cognitive Radio Networks", in *Proc. IEEE INFOCOM*, 2009.